Nanoscale

PAPER

View Article Online
View Journal | View Issue

Cite this: *Nanoscale*, 2016, **8**, 11130

Isolation of atomically precise mixed ligand shell $PdAu_{24}$ clusters†

Annelies Sels,[a] Noelia Barrabés,[b] Stefan Knoppe[c] and Thomas Bürgi*[a]

Received 1st February 2016,
Accepted 26th April 2016

DOI: 10.1039/c6nr00931j

www.rsc.org/nanoscale

Exposure of $PdAu_{24}(2\text{-PET})_{18}$ (2-PET: 2-phenylethylthiolate) to BINAS (1,1-binaphthyl-2,2-dithiol) leads to species of composition $PdAu_{24}(2\text{-PET})_{18-2x}(BINAS)_x$ due to ligand exchange reactions. The BINAS adsorbs in a specific mode that bridges the apex and one core site of two adjacent S(R)–Au–S(R)–Au–S(R) units. Species with different compositions of the ligand shell can be separated by HPLC. Furthermore, site isomers can be separated. For the cluster with exactly one BINAS in its ligand shell only one isomer is expected due to the symmetry of the cluster, which is confirmed by High-Performance Liquid Chromatography (HPLC). Addition of a second BINAS to the ligand shell leads to several isomers. In total six distinguishable isomers are possible for $PdAu_{24}(2\text{-PET})_{14}(BINAS)_2$ including two pairs of enantiomers concerning the adsorption pattern. At least four distinctive isomers are separated by HPLC. Calculations indicate that one of the six possibilities is energetically disfavoured. Interestingly, diastereomers, which have an enantiomeric relationship concerning the adsorption pattern of chiral BINAS, have significantly different stabilities. The relative intensity of the observed peaks in the HPLC does not reflect the statistical weight of the different isomers. This shows, as supported by the calculations, that the first adsorbed BINAS molecule influences the adsorption of the second incoming BINAS ligand. In addition, experiments with the corresponding Pt doped gold cluster reveal qualitatively the same behaviour, however with slightly different relative abundances of the corresponding isomers. This finding points towards the influence of electronic effects on the isomer distribution. Even for clusters containing more than two BINAS ligands a limited number of isomers were found, which is in contrast to the corresponding situation for monothiols, where the number of possible isomers is much larger.

Introduction

Thiolate protected gold nanoclusters $Au_n(SR)_m$ have gained substantial importance[1–3] since the first report on their synthesis.[4] They have attracted considerable attention because of their exceptional size-dependent physical, chemical and optical properties,[5–7] related to their discrete molecular-like electronic structures.[8] Moreover, clusters of certain sizes, the so called 'magic clusters',[9] are highly stable due to their electronic configuration and robust Au–S bond.[10] Stabilized by the thiolate ligands (SR), nanoclusters have attracted interest for various applications.[11–16]

The gold–sulfur interface of thiolate protected clusters is amenable to functionalization,[17] which opens the door for various applications. Encouraged by the pilot work of the Murray group on the kinetics of ligand exchange,[18,19] post-synthetic modification of the clusters *via* ligand exchange reactions is a frequently used method.[20,21] Additionally, kinetic parameters and fundamental information on the clusters and their complex polyfunctional ligand shells can be obtained.[22] Great interest in the exchange mechanism is developing. An associative (SN_2) mechanism is generally accepted and confirmed by Heinecke *et al.*[23] Aikens and co-workers summarized the progress over the last few years, completed by an in-depth theoretical study on the mechanism.[24]

Recently, the influence of hetero-atom doping on ligand exchange reactions, specifically on $Au_{25}(SR)_{18}$, has been thoroughly studied.[25–29] Negishi and co-workers reported an enhancement in the reactivity of $PdAu_{24}(SR)_{18}$ and the separation of ligand exchange products by High-Performance Liquid Chromatography (HPLC) using the step-gradient method.[30,31]

For the use of thiolate protected clusters with mixed ligand shells it might be advantageous to engineer the ligand shell with atomic precision. Towards this goal the isolation of

[a]*Department of Physical Chemistry, University of Geneva, 30 Quai Ernest-Ansermet, 1211 Geneva 4, Switzerland. E-mail: thomas.buergi@unige.ch*
[b]*Institute of Materials Chemistry, Technical University of Vienna, Getreidemarkt 9/BC/01, 1060 Vienna, Austria*
[c]*Molecular Imaging and Photonics, Department of Chemistry, KU Leuven, Celestijnenlaan 200D, 3001 Leuven, Belgium*

†Electronic supplementary information (ESI) available: MALDI mass spectra after 72 h of exchange, CD spectra of clusters after 24 h of exchange, possible exchange isomers of $PdAu_{24}(2\text{-PET})_{14}(R\text{-BINAS})_2$and $PdAu_{24}(2\text{-PET})_{12}(R\text{-BINAS})_3$, and coordinates of the calculated structures. See DOI: 10.1039/c6nr00931j

isomers of mixed ligand shell clusters with identical compositions but differing in the adsorption sites of the thiolates is an interesting though challenging option. It has been shown before for monothiols that such isomers can be separated by HPLC.[32,33] However, monothiols can easily exchange between different places on the clusters. Therefore, a rigid chiral dithiol BINAS (1,1-binaphthyl-2,2-dithiol) was chosen as the substituting ligand.[34] Dithiols may furthermore have the advantage of producing a significantly reduced number of possible exchange products (isomers), compared to monothiols. Furthermore, a higher stability concerning desorption of the ligands is expected. An indication of a possible desorption of monothiols was recently reported by Negishi and coworkers.[33] They observed spontaneous ligand exchange of monothiols between clusters. Such exchange reactions are expected to be less probable for dithiol BINAS. We have recently studied the racemization of chiral $Au_{38}(SR)_{24}$ [35] and found that incorporation of only one BINAS ligand into the ligand shell leads to an increase of the temperature needed to invert the cluster handedness. This shows that BINAS leads to a more rigid Au–S interface.[36] In contrast to $Au_{38}(SR)_{24}$, the original unexchanged $Au_{25}(2\text{-PET})_{18}$ (2-PET: 2-phenylethylthiolate) cluster is achiral. Replacing the original 2-PET ligands by enantiopure R-BINAS is expected to induce chirality.[34]

Structurally, $Au_{25}(SR)_{18}$ consists of a Au_{13} core protected by six dimeric units, or long staples.[37] Each staple represents an –S(R)–Au–S(R)–Au–S(R)– oligomer, containing one apex and two core sulfurs. Calculations indicate an interstaple binding mode of bidentate BINAS,[38] linking the apex S-atom in one staple to a core S-atom in another staple. Considering the distances between the two S-atoms in undistorted BINAS, 4.1 Å, such a binding mode would allow adsorption without large distortion of the molecule, since the distance between the corresponding S-atoms in the cluster is 4.05 Å. Other adsorption modes seem largely unfavourable when considering the mismatch between the S-atoms in BINAS and the corresponding adsorption sites on the cluster. For example, the S-atoms within a staple are separated by about 4.6 Å,[39] whereas the separation between S-atoms at the core positions of two different staples is around 5.05 Å. If the assumption that BINAS only adsorbs in an interstaple mode is correct, then only one isomer is expected for a species with one BINAS in the ligand shell of $Au_{25}(SR)_{18}$ since all possible sites of this type are symmetry equivalent. Furthermore, for species with more than one BINAS ligand a defined and distinguishable number of isomers are expected. This is in contrast to the situation for exchange with mono-thiols, where a huge number of isomers are found. Previous work confirmed the possibility to separate these by HPLC.[32,40]

We performed ligand exchange reactions on $PdAu_{24}(SR)_{18}$ clusters monitored *in situ* by HPLC and succeeded in separation of different exchange products and isomers. An in-depth structural analysis of the exchange isomers completed this study. The obtained results are promising regarding future projects, focussing on the separation of clusters with mixed ligand shells with a precise composition and location of the ligand.

Experimental

Synthesis

All chemicals were used as received without further purification. Nanopure water (18.2 MΩ cm) was used in all experiments that involve water. BINAS was synthesized from BINOL as reported earlier.[22]

Synthesis of monodisperse $PdAu_{24}(2\text{-PET})_{18}$ was performed by following a modified protocol of Pd doped $Au_{38}(SR)_{24}$ clusters.[41]

$HAuCl_4{\cdot}3H_2O$ (1.0 g, 2.54 mmol) and $Na_2PdCl_4{\cdot}3H_2O$ (0.344 g, 0.988 mmol) were dissolved in terahydrofuran (136 mL). 2-PET (1.43 mL, 10.583 mmol) was added to the solution and stirred for 30 min at room temperature. Next, an aqueous solution of $NaBH_4$ (1.54 g, 40.7 mmol, 20 mL) at 0 °C was added to the mixture. The orange suspension soon turned into a black-brown solution, indicating the formation of nanoclusters. After stirring for 3 h, the colorless aqueous phase was removed and the organic phase was filtered to remove insoluble residues. This mixture was dried by using a rotary evaporator and washed with methanol (3 times) to remove 2-PET and other by-products. The products were then dissolved in methylene chloride and passed through a PTFE syringe filter (0.2 μm) to remove insoluble by-products. Acetone extraction results in the removal of larger clusters. The supernatant solution was evaporated, re-dissolved in a minimum amount of toluene and passed over a gel permeation column (GPC, SX1 beads, toluene). At this point $Pd_2Au_{36}(2\text{-PET})_{24}$ is separated from $PdAu_{24}(2\text{-PET})_{18}$. UV-vis analysis confirmed the fraction containing $PdAu_{24}(2\text{-PET})_{18}$ and $Au_{25}(2\text{-PET})_{18}$ (neutral form).

Following the report of Jin *et al.*,[42] the batch was dissolved in 5 mL of DCM. 1 mL H_2O_2 (30 wt%) solution was added every 30 minutes for 2 h to react and selectively decompose the $Au_{25}(2\text{-PET})_{18}$ clusters. After removing the aqueous phase, the organic phase was evaporated and washed with EtOH. The precipitated product was filtered with a Büchner funnel, re-dissolved in DCM and evaporated. Separation with GPC (SX1 beads, toluene) was performed to obtain pure $PdAu_{24}(2\text{-PET})_{18}$ clusters.

Characterization

HPLC separation was performed on a JASCO 20XX HPLC system equipped with a Phenomenex Lux Cellulose-1 column (100 Å, 250 mm × 4.6 mm), and the eluting analytes were detected with a JASCO 2077plus UV detector (420 nm). The analytes were dissolved in toluene and eluted with *n*-hexane : 2-propanol (90 : 10) at a flow rate of 1.75 mL min^{-1}. Mass spectra were recorded on a Bruker Autoflex mass spectrometer equipped with a nitrogen laser at near-threshold laser intensity in positive linear mode using DCTB as the matrix. CD spectra were recorded on a JASCO J-815 CD spectrometer (path length 1 mm, CH_2Cl_2). After 24 h of ligand exchange, the reaction mixture showed a CD-signal (see the ESI†).

Calculations

All computations were carried out using the GPAW software package.[43] The structures considered here were constructed

based on the crystal structure of $[Au_{25}(2\text{-PET})_{18}]^-$.[37] Phenylethanethiolate ligands were replaced by methylthiolate and BINAS was treated as the full ligand. The *S*-enantiomer of BINAS was used in the calculations. Geometry optimizations were run using the LDA functional (h = 0.2 Å, f_{max} = 0.05 eV Å^{-1} on each atom). After geometry optimization, the electronic structure was re-calculated in a single point calculation using the PBE functional on the optimized structures.[44,45]

Linear response TD-DFT calculations were carried out using the PBE functional on a slightly coarser grid (h = 0.25 Å).[46,47] For the ground state calculation, a sufficiently large range of unoccupied states was allowed to converge. Transition energies up to 4.5 eV were considered.

Results and discussion

$PdAu_{24}(SR)_{18}$ clusters were synthesized as the by-products of the $Pd_2Au_{36}(SR)_{24}$ synthesis and isolated by size exclusion chromatography and extraction.[41] After further separation by HPLC, characterization by UV-vis and MALDI-MS ensured the purity of the clusters. Ligand exchange reactions were performed and followed *in situ* similar to that described in previous work.[18] A solution of $PdAu_{24}(SR)_{18}$ (0.5 mg mL^{-1}, toluene) with a 100-fold molar excess of R-BINAS was prepared and injected into the HPLC system every 1.5 h. Similar to the separation method proposed by Negishi *et al.*,[30] a step-gradient mobile phase composition was applied. This step-gradient method allows the clusters to first adsorb onto the stationary phase due to precipitation from MeOH. After substitution of the solvent with a MeOH/THF mixture, the clusters sequentially elute into the mobile phase.

Fig. 1 shows the evolution of the chromatogram of $PdAu_{24}(2\text{-PET})_{18-2x}(BINAS)_x$ (x = 0–4) with time. Only one peak is displayed for $PdAu_{24}(SR)_{18}$ (41 min) and $PdAu_{24}(2\text{-PET})_{16}(R\text{-BINAS})_1$ (44 min).

The initial signal associated with the parent cluster (at 41 min elution time) decreases gradually in intensity, indicating a complete exchange of $PdAu_{24}(SR)_{18}$ after 24 h reaction time. One single peak (retention time 44 min) appears after a short time, increases to a maximum intensity at about 10 h before decreasing and vanishes after around 64 h. Mass spectrometry (Fig. 2) shows that this band corresponds to the first exchange product $PdAu_{24}(2\text{-PET})_{16}(R\text{-BINAS})_1$. The appearance of only one peak is in agreement with the hypothesis discussed above that there is only one possible site where BINAS adsorbs.

The behaviour of this peak in the chromatograms is characteristic of an intermediate in a consecutive reaction, indicating that $PdAu_{24}(2\text{-PET})_{16}(R\text{-BINAS})_1$ is reacting further to give higher exchange products. After extending the reaction time (4.5 h), four new signals (46–50 min) are observed in the chromatogram (Fig. 1) and assigned to $PdAu_{24}(2\text{-PET})_{14}(R\text{-BINAS})_2$ by MALDI mass spectrometry. Obviously at least four distinguishable isomers of this species were formed. A systematic analysis reveals that there are ten principle ways to arrange two BINAS

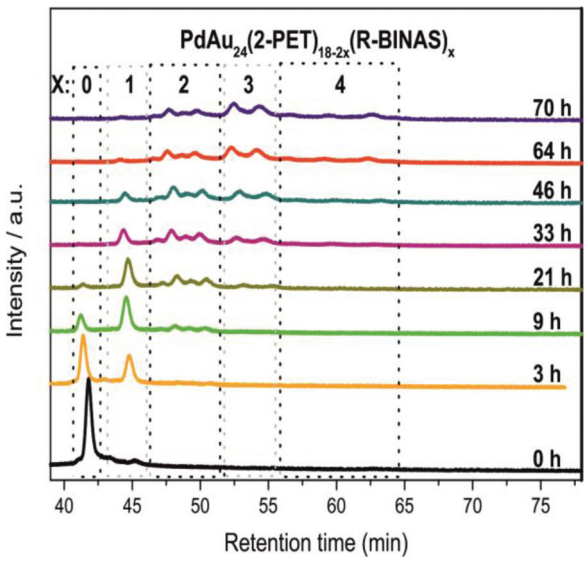

Fig. 1 HPLC chromatogram of $PdAu_{24}(2\text{-PET})_{18-2x}(R\text{-BINAS})_x$ as a function of time. The time indicated is the time between the start of the ligand exchange reaction (addition of BINAS to the cluster solution) and injection of the reaction mixture into the HPLC system.

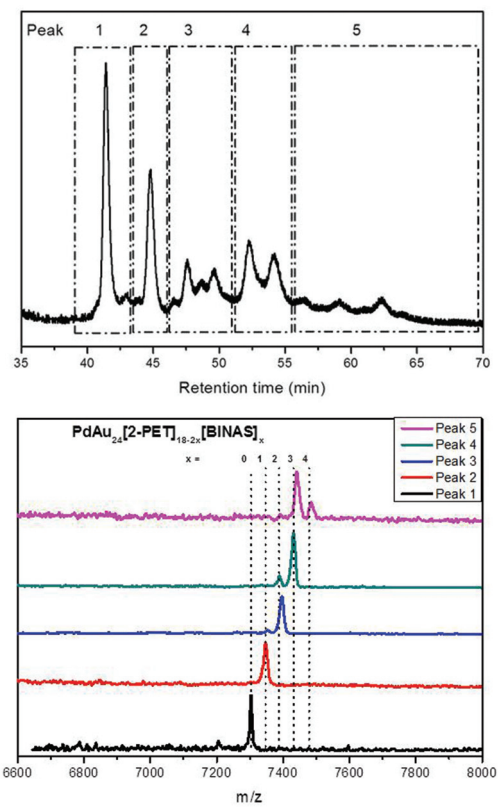

Fig. 2 HPLC chromatogram of the exchanged product (top) and MALDI-TOF mass spectra of each collected fraction (bottom). In order to obtain all species in one HPLC chromatogram, a fresh $PdAu_{24}(2\text{-PET})_{18}$ cluster was added two times in the course of the exchange experiment. Due to slight overlapping of bands in the HPLC separation, MALDI analysis can indicate the presence of a lower exchanged product.

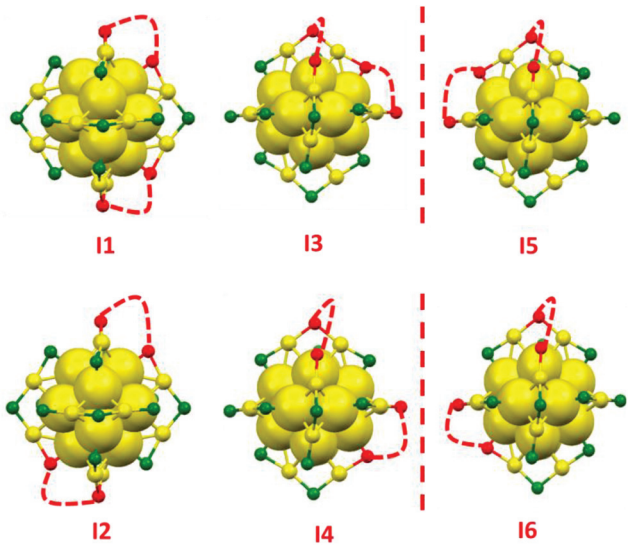

Fig. 3 Isomers of $PdAu_{24}(2\text{-PET})_{14}(R\text{-BINAS})_2$ are shown. The red sulfur atoms and dashed lines indicate the adsorption site of the two BINAS molecules. I3/I5 and I4/I6 are enantiomers concerning the adsorption pattern. However, when considering the chiral BINAS molecule these structures become diastereomers.

molecules on the cluster surface (see the ESI†), however, only six are distinct which we named I1–I6 (Fig. 3). Interestingly, based exclusively on the adsorption pattern of BINAS, two pairs of enantiomers (I3/I5 and I4/I6) can be distinguished (Fig. 3). In consequence, a secondary level of chirality was induced due to the arrangement of the adsorbed BINAS. (Fig. S3†) However, the enantiomeric relationship is destroyed by the chiral BINAS ligands.

Next, DFT calculations were performed in order to find out whether some of the possible isomers are unlikely due to steric constraints arising from interactions between the two BINAS molecules. We used S-BINAS for the calculations but since the cluster is achiral the results are identical to R-BINAS. Note that the Au–S interface of $PdAu_{24}(SR)_{18}$ and its parent cluster $[Au_{25}(SR)_{18}]^-$ has the same structure and therefore the more ubiquitous $[Au_{25}(SR)_{18}]^-$ cluster was considered for the calculations. The relative energies of all isomers were calculated and are listed in Table 1, whereas the corresponding structures are shown in Fig. 4. The calculations revealed isomer I6 as the most stable.

Isomer I5 has considerably higher energy than the other isomers, indicating that the corresponding arrangement of BINAS molecules is hindered. Surprisingly, a large energy difference is observed between I3 and I5, which are enantiomers concerning the adsorption pattern. When considering the structure of BINAS on the cluster, I3 and I5 become diastereomers. The orientation of ligands in I5, imposed by the chiral adsorption pattern, increases the steric hindrance and therefore the energy of this isomer with respect to I3. It should be noted that the calculations neglect both solvent and ligand (2-PET) interactions, which can influence the relative energy of the cluster isomers. In consequence, out of the six possible

Table 1 Isomers of $[Au_{25}(SCH_3)_{18-2x}(S\text{-BINAS})_x]^-$, their degeneracies g_i (representing the number of ways to construct the same cluster from different numbered exchange sites, see the ESI) and relative energies. All values refer to PBE single point calculations on LDA optimized structures

Cluster	Isomer	g_i	E_{rel}/eV
$[Au_{25}(SCH_3)_{18}]^-$	—	1	0.00
$[Au_{25}(SCH_3)_{16}(BINAS)_1]^-$	—	1	0.00
$Au_{25}(SCH_3)_{14}(BINAS)_2]^-$	I1[a]	1	0.16
	I2[a]	1	0.14
	I3[a]	2	0.07
	I4[b]	2	0.08
	I5	2	0.54
	I6[c]	2	0.00

[a] Absolute configuration at the apex atom is inverted. [b] Absolute configuration at the core atom is inverted. [c] Absolute configuration of both apex and core site atoms is inverted. The inversions refer to the incorporation of the second BINAS ligand.

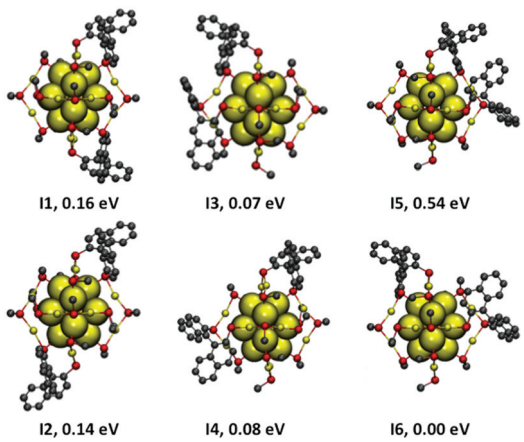

Fig. 4 Optimized structures of $[Au_{25}(SCH_3)_{14}(S\text{-BINAS})_2]^-$.

structures one structure seems highly destabilized, as indicated by the calculations, due to unfavourable interactions between the two adsorbed BINAS molecules. In the chromatograms only four bands that are assigned to $PdAu_{24}(2\text{-PET})_{14}(R\text{-BINAS})_2$ are observed. Possible explanations are that two isomers have the same retention time or that one isomer has too low abundance to be observed.

Niihori *et al.* reported a comparable separation of coordination isomers using HPLC after ligand exchange by monothiols.[33] An unequal isomer distribution due to the preferential core sulfur exchange site was observed. Additionally, they observed statistical behaviour of the exchange after some time, indicating that in their case the different isomers have merely the same energy. It seems that in our case the situation is different. We observe four bands in the chromatograms associated with $PdAu_{24}(2\text{-PET})_{14}(R\text{-BINAS})_2$ isomers with different intensities and relative ratios. Interestingly these relative ratios do not change with time. The relative intensities do not fit with the degeneracies emerging from the systematic analysis of the possible isomers, which indicates that the rela-

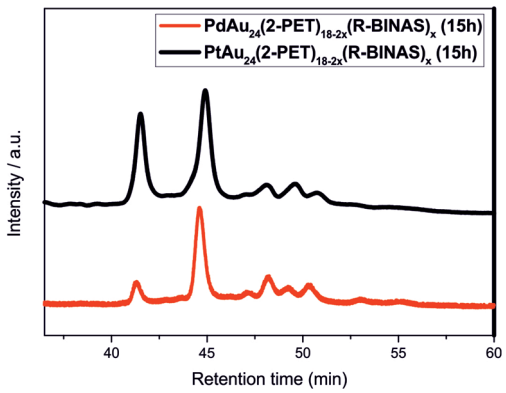

Fig. 5 HPLC chromatograms after exchange of $PdAu_{24}(2\text{-}PET)_{18-2x}(R\text{-}BINAS)_x$ and $PtAu_{24}(2\text{-}PET)_{18-2x}(R\text{-}BINAS)_x$.

tive abundance of the isomers is not statistical. Therefore, the first adsorbed BINAS molecule, to some extent, influences the adsorption site of the second incoming BINAS molecule.

To support the findings discussed above the same ligand exchange reaction was performed on $PtAu_{24}(2\text{-}PET)_{18-2x}(R\text{-}BINAS)_x$. Hence with the structural similarities of Pd and Pt doped $Au_{25}(2\text{-}PET)_{18}$ clusters, an identical exchange behaviour is predicted. As expected, the chromatograms of both the doped clusters (Fig. 5) show similar separation of exchange products, with slightly different relative intensities. Since the two heteroatoms are located in the centre of the cluster without direct contact with the ligands,[48,49] this finding indicates that electronic effects can influence the relative stability of coordination isomers.

Increasing the reaction time, new peaks appear at higher retention times (Fig. 1). Continuing on the previous line of reasoning, these signals can be assigned to the third and fourth exchange of BINAS, as confirmed by MALDI mass spectrometry. Systematic analysis reveals in total 15 different isomers for $PdAu_{24}(2\text{-}PET)_{12}(R\text{-}BINAS)_3$. Considering that the relative arrangement of two BINAS molecules as for isomer I5 in Fig. 4 is energetically disfavoured reduces this number to seven (see the ESI†). In the HPLC traces there are two major bands that can be associated with $PdAu_{24}(2\text{-}PET)_{12}(R\text{-}BINAS)_3$ at 53–55 min retention time. The true nature of higher retained products (>57 min RT) could not be clarified due to unclear separation. Peak 5 collected in the HPLC (Fig. 2) contains several smaller bands. The corresponding MALDI trace shows a mixture of $PdAu_{24}(2\text{-}PET)_{12}(R\text{-}BINAS)_3$ and $PdAu_{24}(2\text{-}PET)_{10}(R\text{-}BINAS)_4$ with a maximum for $x = 3$. Therefore the former cluster contains additional isomers besides the two major ones collected in band 4 (Fig. 2).

Conclusions

In summary, we were able to separate different exchange products and isomers of $PdAu_{24}(2\text{-}PET)_{18-2x}(R\text{-}BINAS)_x$. The results indicate that BINAS adsorbs selectively on a site that bridges the core and the apex of two adjacent staples. Although twelve such sites exist on the cluster only one isomer is formed for $PdAu_{24}(2\text{-}PET)_{16}(R\text{-}BINAS)_1$ because all sites are symmetry equivalent. For $PdAu_{24}(2\text{-}PET)_{14}(R\text{-}BINAS)_2$ six isomers are possible but calculations indicate that one isomer is strongly disfavoured. At least four isomers were identified by HPLC separation. A secondary level of chirality arises in some of the clusters from the adsorption pattern of the substituted ligands. In contrast to the statistical isomer distribution found for monothiols,[33] a preferential exchange pattern was observed, which can presumably be assigned to interactions between the adsorbed BINAS dithiolate and/or to the structural distortion of the cluster. Similar exchange behaviour was observed for $PtAu_{24}(2\text{-}PET)_{18}$ and is also expected for monometallic $Au_{25}(2\text{-}PET)_{18}$. However, the different relative abundance of the isomers of the Pd and Pt doped clusters points towards the importance of electronic effects. Isolation of different place isomers is expected to be interesting for future use as atomically precise nanoscale entities. In this respect rigid dithiolates as the one used here may have advantages over monothiolates due to the fewer number of possible isomers and lower probability that the entities move on the cluster surface and between the clusters.

Acknowledgements

S. K. is a postdoctoral fellow of the Funds for Scientific Research – Flanders (FWO). All computations were carried out at 'CSC – The IT Center for Science' (Espoo, Finland).

N. B. acknowledges support by the Swiss National Science Foundation under the Marie Heim-Vögtlin grant (PMPDP2_145512). Funding from the Swiss National Science Foundation (grant number 200020-152596) is acknowledged. We thank Bei Zhang for helpful scientific discussions.

References

1 H. Hakkinen, *Nat. Chem.*, 2012, **4**, 443–455.
2 R. Jin, *Nanoscale*, 2015, **7**, 1549–1565.
3 P. Maity, S. Xie, M. Yamauchi and T. Tsukuda, *Nanoscale*, 2012, **4**, 4027–4037.
4 M. Brust, M. Walker, D. Bethell, D. J. Schiffrin and R. Whyman, *J. Chem. Soc., Chem. Commun.*, 1994, 801–802, DOI: 10.1039/C39940000801.
5 H. Qian, M. Zhu, Z. Wu and R. Jin, *Acc. Chem. Res.*, 2012, **45**, 1470–1479.
6 M. Zhu, C. M. Aikens, F. J. Hollander, G. C. Schatz and R. Jin, *J. Am. Chem. Soc.*, 2008, **130**, 5883–5885.
7 M. M. Alvarez, J. T. Khoury, T. G. Schaaff, M. N. Shafigullin, I. Vezmar and R. L. Whetten, *J. Phys. Chem. B*, 1997, **101**, 3706–3712.
8 Y. Negishi, T. Nakazaki, S. Malola, S. Takano, Y. Niihori, W. Kurashige, S. Yamazoe, T. Tsukuda and H. Häkkinen, *J. Am. Chem. Soc.*, 2015, **137**, 1206–1212.

9 Y. Negishi, Y. Takasugi, S. Sato, H. Yao, K. Kimura and T. Tsukuda, *J. Am. Chem. Soc.*, 2004, **126**, 6518–6519.
10 Y. Negishi, K. Nobusada and T. Tsukuda, *J. Am. Chem. Soc.*, 2005, **127**, 5261–5270.
11 P. K. Jain, X. Huang, I. H. El-Sayed and M. A. El-Sayed, *Acc. Chem. Res.*, 2008, **41**, 1578–1586.
12 N. Shukla, M. A. Bartel and A. J. Gellman, *J. Am. Chem. Soc.*, 2010, **132**, 8575–8580.
13 Z. Wu, D.-e. Jiang, A. K. P. Mann, D. R. Mullins, Z.-A. Qiao, L. F. Allard, C. Zeng, R. Jin and S. H. Overbury, *J. Am. Chem. Soc.*, 2014, **136**, 6111–6122.
14 W. Chen and S. Chen, *Angew. Chem., Int. Ed.*, 2009, **48**, 4386–4389.
15 Y. Zhu, H. Qian and R. Jin, *J. Mater. Chem.*, 2011, **21**, 6793–6799.
16 Y. Lu, Y. Jiang, X. Gao and W. Chen, *Chem. Commun.*, 2014, **50**, 8464–8467.
17 T. Burgi, *Nanoscale*, 2015, **7**, 15553–15567.
18 R. Guo, Y. Song, G. Wang and R. W. Murray, *J. Am. Chem. Soc.*, 2005, **127**, 2752–2757.
19 A. Dass, K. Holt, J. F. Parker, S. W. Feldberg and R. W. Murray, *J. Phys. Chem. C*, 2008, **112**, 20276–20283.
20 V. R. Jupally, R. Kota, E. V. Dornshuld, D. L. Mattern, G. S. Tschumper, D.-e. Jiang and A. Dass, *J. Am. Chem. Soc.*, 2011, **133**, 20258–20266.
21 E. S. Shibu, M. A. H. Muhammed, T. Tsukuda and T. Pradeep, *J. Phys. Chem. C*, 2008, **112**, 12168–12176.
22 S. Knoppe, R. Azoulay, A. Dass and T. Bürgi, *J. Am. Chem. Soc.*, 2012, **134**, 20302–20305.
23 C. L. Heinecke, T. W. Ni, S. Malola, V. Mäkinen, O. A. Wong, H. Häkkinen and C. J. Ackerson, *J. Am. Chem. Soc.*, 2012, **134**, 13316–13322.
24 A. Fernando and C. M. Aikens, *J. Phys. Chem. C*, 2015, **119**, 20179–20187.
25 Y. Negishi, W. Kurashige, Y. Niihori, T. Iwasa and K. Nobusada, *Phys. Chem. Chem. Phys.*, 2010, **12**, 6219–6225.
26 C. Kumara, C. M. Aikens and A. Dass, *J. Phys. Chem. Lett.*, 2014, **5**, 461–466.
27 Y. Negishi, K. Munakata, W. Ohgake and K. Nobusada, *J. Phys. Chem. Lett.*, 2012, **3**, 2209–2214.
28 W. Kurashige, K. Munakata, K. Nobusada and Y. Negishi, *Chem. Commun.*, 2013, **49**, 5447–5449.
29 Y. Niihori, W. Kurashige, M. Matsuzaki and Y. Negishi, *Nanoscale*, 2013, **5**, 508–512.
30 Y. Niihori, M. Matsuzaki, C. Uchida and Y. Negishi, *Nanoscale*, 2014, **6**, 7889–7896.
31 Y. Niihori, M. Matsuzaki, T. Pradeep and Y. Negishi, *J. Am. Chem. Soc.*, 2013, **135**, 4946–4949.
32 L. Beqa, D. Deschamps, S. Perrio, A.-C. Gaumont, S. Knoppe and T. Bürgi, *J. Phys. Chem. C*, 2013, **117**, 21619–21625.
33 Y. Niihori, Y. Kikuchi, A. Kato, M. Matsuzaki and Y. Negishi, *ACS Nano*, 2015, **9**, 9347–9356.
34 S. Knoppe and T. Burgi, *Phys. Chem. Chem. Phys.*, 2013, **15**, 15816–15820.
35 S. Knoppe, I. Dolamic and T. Bürgi, *J. Am. Chem. Soc.*, 2012, **134**, 13114–13120.
36 S. Knoppe, S. Michalet and T. Bürgi, *J. Phys. Chem. C*, 2013, **117**, 15354–15361.
37 M. W. Heaven, A. Dass, P. S. White, K. M. Holt and R. W. Murray, *J. Am. Chem. Soc.*, 2008, **130**, 3754–3755.
38 B. Molina, A. Sanchez-Castillo, S. Knoppe, I. L. Garzon, T. Burgi and A. Tlahuice-Flores, *Nanoscale*, 2013, **5**, 10956–10962.
39 H. Qian, W. T. Eckenhoff, Y. Zhu, T. Pintauer and R. Jin, *J. Am. Chem. Soc.*, 2010, **132**, 8280–8281.
40 Y. Niihori, C. Uchida, W. Kurashige and Y. Negishi, *Phys. Chem. Chem. Phys.*, 2016, **18**, 4251–4265.
41 N. Barrabés, B. Zhang and T. Bürgi, *J. Am. Chem. Soc.*, 2014, **136**, 14361–14364.
42 H. Qian, D.-e. Jiang, G. Li, C. Gayathri, A. Das, R. R. Gil and R. Jin, *J. Am. Chem. Soc.*, 2012, **134**, 16159–16162.
43 J. Enkovaara, C. Rostgaard, J. J. Mortensen, J. Chen, M. Dułak, L. Ferrighi, J. Gavnholt, C. Glinsvad, V. Haikola, H. A. Hansen, H. H. Kristoffersen, M. Kuisma, A. H. Larsen, L. Lehtovaara, M. Ljungberg, O. Lopez-Acevedo, P. G. Moses, J. Ojanen, T. Olsen, V. Petzold, N. A. Romero, J. Stausholm-Møller, M. Strange, G. A. Tritsaris, M. Vanin, M. Walter, B. Hammer, H. Häkkinen, G. K. H. Madsen, R. M. Nieminen, J. K. Nørskov, M. Puska, T. T. Rantala, J. Schiøtz, K. S. Thygesen and K. W. Jacobsen, *J. Phys.: Condens. Matter*, 2010, **22**, 253202.
44 J. P. Perdew, K. Burke and M. Ernzerhof, *Phys. Rev. Lett.*, 1996, **77**, 3865–3868.
45 J. P. Perdew, K. Burke and M. Ernzerhof, *Phys. Rev. Lett.*, 1997, **78**, 1396–1396.
46 S. Malola, L. Lehtovaara, S. Knoppe, K.-J. Hu, R. E. Palmer, T. Bürgi and H. Häkkinen, *J. Am. Chem. Soc.*, 2012, **134**, 19560–19563.
47 H. Yang, Y. Wang, H. Huang, L. Gell, L. Lehtovaara, S. Malola, H. Häkkinen and N. Zheng, *Nat. Commun.*, 2013, **4**, 2422.
48 S. L. Christensen, M. A. MacDonald, A. Chatt, P. Zhang, H. Qian and R. Jin, *J. Phys. Chem. C*, 2012, **116**, 26932–26937.
49 M. A. Tofanelli, T. W. Ni, B. D. Phillips and C. J. Ackerson, *Inorg. Chem.*, 2016, **55**, 999–1001.